ADVANCED ENERGY MATERIALS

www.advenergymat.de

Significantly Enhancing the Efficiency of a New Light-Harvesting Polymer with Alkylthio naphthyl Substituents Compared to Their Alkoxyl Analogs

Gongyue Huang, Jun Zhang, Nergui Uranbileg, Weichao Chen, Huanxiang Jiang, Hua Tan, Weiguo Zhu,* and Renqiang Yang**

In this work, a new benzo[1,2-*b*:4,5-*b*′]dithiophene (BDT) building block containing alkylthio naphthyl as a side chain is designed and synthesized, and the resulting polymer, namely PBDTNS-BDD, shows a lower HOMO energy level than that of its alkoxyl naphthyl counterpart PBDTNO-BDD. An optimized photovoltaic device using PBDTNS-BDD as a donor exhibits power conversion efficiencies (PCE) of 8.70% and 9.28% with the fullerene derivative $PC_{71}BM$ and the fullerene-free small molecule ITIC as acceptors, respectively. Surprisingly, ternary blend devices based on PBDTNS-BDD and two acceptors, namely $PC_{71}BM$ and ITIC, shows a PCE of 11.21%, which is much higher than that of PBDTNO-BDD based ternary devices (7.85%) even under optimized conditions.

Polymer solar cells have been widely investigated because of their flexibility, light weight, low production cost, and suitability for large-scale production.[1–4] Recently, the power conversion efficiencies (PCEs) of state-of-the-art polymer solar cells have already surpassed 12% for single-junction devices, which can mainly be ascribed to the innovation of photoactive materials and device structures, especially, the emergence of fullerene-free acceptors and ternary blend solar cells based on three active components with complementary absorption spectra.[5–8] At present, the design and synthesis of new solution-processed polymers with appropriate cascade energy levels and complementary absorption to fabricate ternary blend organic solar cells is a vitally important approach to obtain high PCEs.

The PCE of polymer solar cells is determined by three parameters, namely, the open-circuit voltage (V_{OC}), the short-circuit current density (J_{SC}), and the fill factor (FF). A low-lying highest occupied molecular orbital (HOMO) energy level is essential for donor materials to achieve a high V_{OC}, although the V_{OC} is mainly dependent on the offset between the HOMO energy level of the donor and the lowest unoccupied molecular orbital (LUMO) energy level of the acceptor.[9,10] On the other hand, appropriate and matching energy levels of the donor and the acceptor are indispensable for efficient exciton dissociation to obtain a higher J_{SC}. Also indispensable for achieving a higher J_{SC} is that the active materials have a broad and strong absorption within the visible and near-infrared regions in order to harvest more photons. However, the absorption spectrum of binary devices tends to exhibit weak absorption in certain regions, which results in the ineffective use of photons.[11–13] Moreover, enhancing the inter-molecular π–π stacking could improve the J_{SC} and FF because of the increasing charge-carrier transport. Therefore, developing a new strategy to design efficient materials for high-performance polymer solar cells is still crucial.

Benzo[1,2-b:4,5-b′]dithiophene (BDT), the most popular donor building block, has been widely employed to construct high-efficiency, light-harvesting polymers because of its planar and symmetrical molecular structure.[14–22] In general, conjugated polymers based on two-dimensional (2D)-BDT usually have a superior device performance than their 1D counterparts.[23] With the incorporation of π-conjugated side chains like thienyl or phenyl groups, the monomers can extend vertical conjugation and further strengthen the π–π stacking, thus charge-carrier transport could be more efficient and the photovoltaic performance could be better. Moreover, the 2D side chain in the BDT unit can be easily modified by the introduction of heteroatoms like O or S.[24–28] Especially, the introduction of sulfur can slightly red-shift the absorption of the

G. Huang, J. Zhang, N. Uranbileg, Dr. W. Chen, H. Jiang, Prof. R. Yang
CAS Key Laboratory of Bio-based Materials
Qingdao Institute of Bioenergy and Bioprocess Technology
Chinese Academy of Sciences
Qingdao 266101, P. R. China
E-mail: chenwc@qdu.edu.cn; yangrq@qibebt.ac.cn
Dr. W. Chen
College of Textiles & Clothing
Qingdao University
Qingdao 266071, P. R. China
Prof. W. Zhu
School of Materials Science and Engineering
Changzhou University
Changzhou 213164, P. R. China
E-mail: zhuwg18@126.com
G. Huang, J. Zhang, Dr. H. Tan, Prof. W. Zhu
College of Chemistry
Xiangtan University
Xiangtan 411105, P. R. China
The ORCID identification number(s) for the author(s) of this article can be found under https://doi.org/10.1002/aenm.201702489.

DOI: 10.1002/aenm.201702489

polymer and down-shift the HOMO energy level, resulting in a deeper HOMO and better device performance. Currently, the 2D-BDT monomers containing thiophene, thieno [3,2-b]thiophene, benzene, biphenyl and their thio- compounds, are being studied widely by many groups.[29–33] Compared to these reported side chains, the naphthalene unit exhibits bigger π-conjugation and better planarity.[34] These features ensure that incorporation of the naphthalene group can extend conjugation and increase π–π stacking. However, studies on the fused naphthalene ring are rare. And to our knowledge, there have been no reports on the BDT monomer being substituted by the alkylthio naphthyl side chain.

In addition, to develop highly efficient photoactive materials, device optimization is also crucially important. Recently, ternary-blend polymer solar cells have been regarded as a simple and effective strategy to extend the photo-response and thus improve the PCE in single-junction devices by several groups.[35–37] Ternary-blend organic solar cells can be composed of either two donors/one acceptor (D1:D2:A) or one donor/two acceptors (D:A1:A2). $PC_{71}BM$ and ITIC have been widely used as the most popular acceptor materials. The former shows the advantages of high electron mobility, large electron affinity and charge transport isotropy. The latter features a high absorptivity and high LUMO energy level. However, their shortcomings are also apparent. $PC_{71}BM$ exhibits a weak absorption in the visible region and a relatively low-lying LUMO energy level which results in large energy losses. ITIC has a low electron mobility and bad film morphology due to strong aggregation of the small molecules. It has been shown to be feasible to integrate $PC_{71}BM$ and ITIC as an "alloy" acceptor to effectively synergize their advantages and make up for their deficiencies.[38–40] Further research has found that the bimolecular recombination and the trap assistant recombination in the ternary blend film could be reduced, which simultaneously improved the J_{SC}, V_{OC}, and PCE.[41]

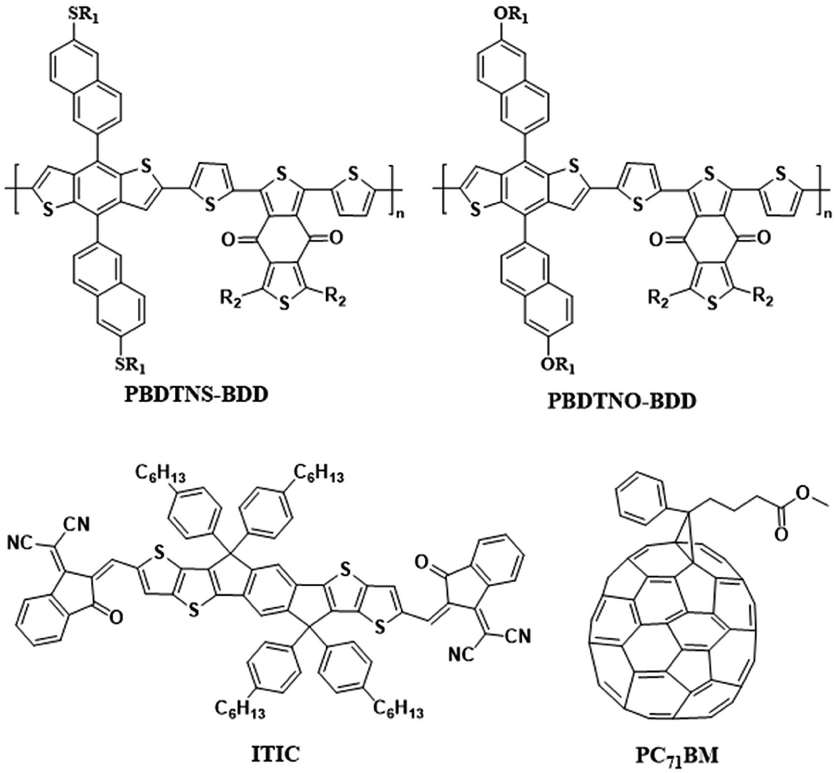

Figure 1. Chemical structures of the polymers and acceptors.

In this work, a new 2D-BDT monomer with alkylthio naphthyl as a side chain (BDTNS, Scheme S1, Supporting Information) was designed and synthesized. The target polymer named PBDTNS-BDD, was obtained using a Pd-catalyzed Stille coupling reaction between the 1,3-bis(5-bromothiophen-2-yl)-5,7-bis(2-ethylhexyl)-4H,8H-benzo[1,2-c:4,5-c′]dithiophene-4,8-dione (BDD) unit and the monomer BDTNS. Meanwhile, the analogous polymer with alkoxyl naphthyl as a side chain, named PBDTNO-BDD, was also synthesized for comparison. The chemical structures of the polymers and acceptors used in this work are shown in **Figure 1**. The detailed synthetic procedure and structural characterization can be found in the Supporting Information.

The two polymers both exhibited a good thermal stability, low HOMO energy level, and broad absorption. PBDTNS-BDD and PBDTNO-BDD showed an onset decomposition temperature (T_d) with 5% weight loss at 379°C and 412°C (Figure S1, Supporting Information), respectively. The absorption of the polymers was examined. PBDTNS-BDD showed similar absorption profiles both in o-dichlorobenzene solution and in the solid film (**Figure 2** and Figure S2, Supporting Information) to those of PBDTNO-BDD. This indicated that the alkylthio naphthyl unit did not lead to a blue-shift in absorption as opposed to the widely reported alkylthio thiophene system, which would be conducive to harvest a larger fraction of the solar spectrum.[24,27] The optical bandgaps of PBDTNS-BDD and PBDTNO-BDD were around 1.81 eV and 1.83 eV, respectively, which were estimated from the absorption edge of the films. The UV–vis spectra of the two polymers in film were both red-shifted by 15 nm compared to that in solution, indicating that they exhibited moderate aggregation behavior. The main peak at 580 nm could be assigned to the intramolecular charge transfer (ICT) interaction in D–A systems. Interestingly, the PBDTNS-BDD polymer showed stronger ICT effects than those of PBDTNO-BDD (Figure 2a). Together with its slightly wider absorption spectra, this implies that PBDTNS-BDD would be a more promising wide-bandgap, light-harvesting polymer and probably would have a higher photovoltaic performance.

The electrochemical properties of PBDTNS-BDD and PBDTNO-BDD were measured by cyclic voltammetry (CV). As shown in Figure S3 (Supporting Information), the onset oxidation potentials of PBDTNS-BDD and PBDTNO-BDD were 1.01 V and 0.93 V, respectively, corresponding to a HOMO energy level of −5.35 eV and −5.27 eV, respectively. The LUMO energy levels derived from the HOMO levels and the optical

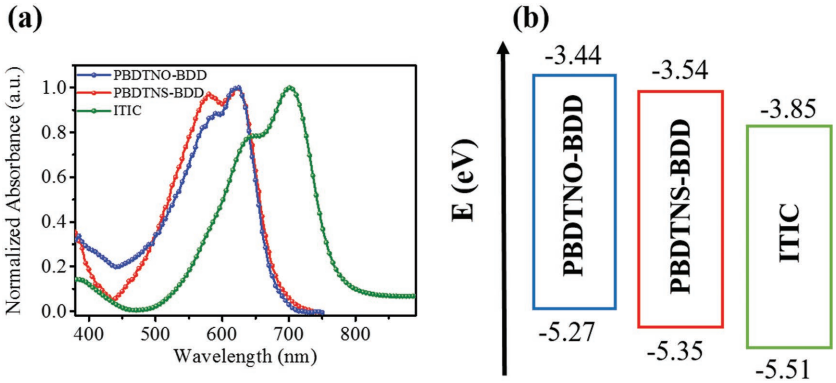

Figure 2. a) UV–vis absorption spectra in film. b) Energy diagram of PBDTNS-BDD, PBDTNO-BDD, and ITIC.

bandgap were about −3.54 eV and −3.44 eV. And, as expected, the HOMO level of PBDTNS-BDD was 0.08 eV lower compared to that of PBDTNO-BDD, confirming that the alkylthio naphthyl side chain in 2D-conjugated copolymers can significantly influence the electronic properties of polymers. According to the absorption and lowered HOMO level, it can be inferred that PBDTNS-BDD would show a superior performance in PSCs compared to its alkoxyl analogue PBDTNO-BDD.

The photovoltaic properties of the two polymers were investigated. Two types of binary bulk heterojunction devices based on either of the polymers as the donor and $PC_{71}BM$ or ITIC as acceptor were constructed. The device was optimized by changing the weight ratio of the donor to acceptor (D/A, w/w) in the active layer with a conventional structure of ITO/PEDOT:PSS/donor:acceptor/PFN/Al. The current density (*J*) versus voltage (*V*) curves of all the devices with different D/A ratios are shown in Figure S4 (Supporting Information). The optimal photovoltaic parameters are summarized in **Table 1** and the corresponding *J*–*V* curves are shown in **Figure 3**. It can be seen that the PBDTNS-BDD based devices showed a better performance than that of the PBDTNO-BDD based devices. With the typical fullerene derivative $PC_{71}BM$ as an acceptor, the PBDTNS-BDD based devices showed an optimal PCE of 8.70%, at a V_{OC} of 0.91 V, a J_{SC} of 12.89 mA cm^{-2}, and a FF of 74.23%, which are all higher than those of the PBDTNO-BDD based devices with a PCE of only 6.64% (V_{OC} = 0.85 V, J_{SC} = 12.06 mA cm^{-2}, and FF = 64.81%).

Recently the fullerene-free acceptor ITIC has attracted great attention and some breakthroughs in efficiency have been obtained, which could be mainly ascribed to the higher V_{OC} of the devices based on ITIC than that of the devices based on fullerene. Moreover, ITIC shows a strong absorption in the near-infrared region, which can generate a larger J_{SC}. As expected, with ITIC as the acceptor, the PBDTNS-BDD-based devices showed a higher V_{OC} (0.94 V) and J_{SC} (14.86 mA cm^{-2}) than those of the PBDTNS-BDD/$PC_{71}BM$ devices, resulting in a better PCE of 9.28% (Figure 3a and Table 1). The PBDTNO-BDD devices with ITIC as the acceptor exhibited a similar enhancement (V_{OC} = 0.87 V, J_{SC} = 13.49 mA cm^{-2}, and PCE = 7.05%) compared to the devices with $PC_{71}BM$ as acceptor. The photo-response properties of all devices were examined. The corresponding external quantum efficiency (EQE) spectra are shown in Figure 3b. It can be clearly seen that when ITIC was employed as the acceptor, the binary blend devices exhibited a much broader photo-response range, extending from 700 nm to 800 nm, than that of the $PC_{71}BM$-based devices. As a result, a larger J_{SC} was obtained (Table 1, Figure S4, Supporting Information). It is clear that the enhancement of J_{SC} was due to the ITIC, as this has a strong absorption between 700–800 nm (Figure 2a).

Compared to PBDTNO-BDD, the better performance of the PBDTNS-BDD-based devices mainly benefitted from the higher V_{OC} (0.91 V vs. 0.85 V for $PC_{71}BM$, and 0.94 V vs. 0.87 V for ITIC). And the lower HOMO level of the PBDTNS-BDD contributed to the higher V_{OC} of these devices. This indicated that the alkylthio naphthyl substituent played an important role in decreasing the HOMO level and therefore increasing the V_{OC} of the devices compared to the alkoxyl naphthyl analogue. The high FF also made a substantial contribution to the high performance of the PBDTNS-BDD-based devices, which may result from the relatively balanced charge-carrier transport. The transport characteristics were investigated using a space charge-limited current model to measure the hole and electron mobilities in the blend films. The *J*–*V* curves are shown in Figure S5 in the Supporting Information. In both binary blend films, PBDTNS-BDD displayed relatively higher hole mobilities than those in the PBDTNO-BDD film, as shown in Table S1 (Supporting Information). Smaller ratios of the electron to hole mobility (μ_e/μ_h) of 0.90 and 1.58 (closer to 1) were obtained for PBDTNS-BDD:$PC_{71}BM$ and PBDTNS-BDD:ITIC blends, respectively, compared to those of the PBDTNO-BDD blends (2.44 and 6.46 for $PC_{71}BM$ and ITIC, respectively). Therefore, a more balanced charge-carrier transport in the PBDTNS-BDD blends may be one of the reasons for the higher FF.[42]

Considering the exactly complementary absorption spectra and appropriate energy levels (Figure 2), ternary blend organic solar cells were fabricated employing one of the polymers as donor and $PC_{71}BM$ and ITIC as the two acceptors. The cells were optimized by changing the ratio of ITIC to $PC_{71}BM$. The *J*–*V* curves of the ternary blend devices with different ratios

Table 1. The photovoltaic parameters of the devices.

Device	V_{OC} [V]	J_{SC} [mA cm^{-2}][a)]	FF [%]	PCE [%][b)]
PBDTNO-BDD:$PC_{71}BM$	0.85	12.06 (11.46)	64.81	6.64(6.50)
PBDTNO-BDD:ITIC	0.87	13.49 (13.12)	60.05	7.05(6.89)
PBDTNO-BDD: Ternary	0.85	15.36 (14.96)	60.13	7.85(7.73)
PBDTNS-BDD:$PC_{71}BM$	0.91	12.89 (11.83)	74.23	8.70(8.61)
PBDTNS-BDD:ITIC	0.94	14.86 (14.02)	66.47	9.28(9.18)
PBDTNS-BDD: Ternary	0.93	17.77 (17.12)	67.81	11.21(11.13)

[a)]Integrated J_{SC} from EQE spectra of the best device in brackets, [b)]The average PCE in parentheses were obtained from 15 devices.

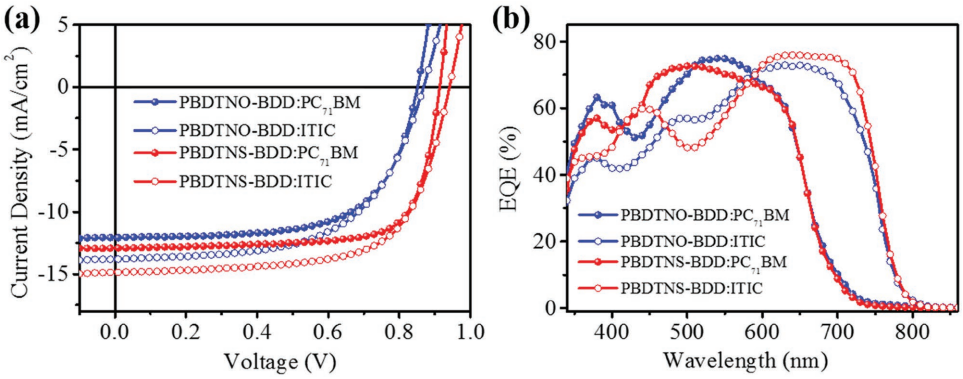

Figure 3. a) *J–V* curves of the optimal binary devices. b) EQE spectra of the corresponding binary devices.

of ITIC to $PC_{71}BM$ are shown in Figure S7 (Supporting Information), and the corresponding photovoltaic parameters are summarized in Table S2 in the Supporting Information. As shown in Table S2, the ternary devices can retain a relative stable performance even when the ratios of the two acceptors vary in a large range. It suggests that this ternary system can be very robust without the need for precise control of the blending ratio and would have a wide range of potential applications. For the PBDTNS-BDD-based devices, an optimal PCE of 11.21% was achieved with a V_{OC} of 0.93 V, a J_{SC} of 17.77 mA cm^{-2}, and a FF of 67.81% for a blend ratio of 1:1.2:0.3 (PBDTNS-BDD:ITIC:$PC_{71}BM$) as shown in **Figure 4** and Table 1. This was much higher than that of the PBDTNO-BDD-based ternary devices (PCE only 7.85%). Compared to the two PBDTNS-BDD-based binary blend devices, the performance of the ternary devices showed a surprising improvement, which was mainly due to the higher J_{SC}. As show in Figure 3b, the PBDTNS-BDD:ITIC binary device exhibited a broader photoresponse in the long wavelength range but lower EQE values in the short wavelength range than the PBDTNS-BDD:$PC_{71}BM$ binary device. Interestingly, the addition of a small amount of $PC_{71}BM$ into the PBDTNS-BDD: ITIC blend as the third component effectively improved the photo-response intensity at a wavelength of around 500 nm. A calculated current density of 17.12 mA cm^{-2} was obtained by integrating the EQE curve with the standard solar spectrum (AM 1.5G), which was consistent with the measured J_{SC} with an error of <5%. The saturation current density (J_{sat}) was about 18.53 mA cm^{-2}, which was calculated by fitting the curve of the net photocurrent and the effective applied voltage as shown in Figure 4c. A ratio J_{ph}/J_{sat} of 94% under short-circuit conditions indicates that the photogenerated excitons were efficiently dissociated into free holes and electrons, and then collected substantially at the electrodes with little recombination.[43] The power-law dependence of J_{SC} on the light intensity (P), J_{SC} versus P^{α} is shown in the inset of Figure 4c. It clearly shows that the value of α approaches 1, which means that little bimolecular recombination occurred in the ternary system. On the other hand, the hole and electron mobilities were about 1.99×10^{-4} cm^2 V^{-1} s^{-1} and 8.99×10^{-5} cm^2 V^{-1} s^{-1} with a μ_h/μ_e of 2.21 as shown in Figure S8 (Supporting Information), which partly suggests that the low recombination rate may come from the relatively balanced charge-carrier transport.

The morphology of the active layer usually plays a significant role in the device performance. The morphologies of the blend films at optimized conditions were investigated by atomic force microscopy (AFM) and transmission electron microscopy (TEM). The two polymers blended with $PC_{71}BM$ showed a smooth surface (root-mean-square (RMS) roughness of <2 nm) and a uniform fabric-like microstructure (Figure S6a,b,e,f), indicating that the polymers exhibited a good miscibility with $PC_{71}BM$. However, when blending with ITIC, both exhibited a fairly rough surface (RMS = 6.4 nm and 5.7 nm for PBDTNS-BDD and PBDTNO-BDD blends, respectively) and obvious aggregated micro-domains (Figure S6c,d,g,h), implying that the excitons may not be efficiently separated

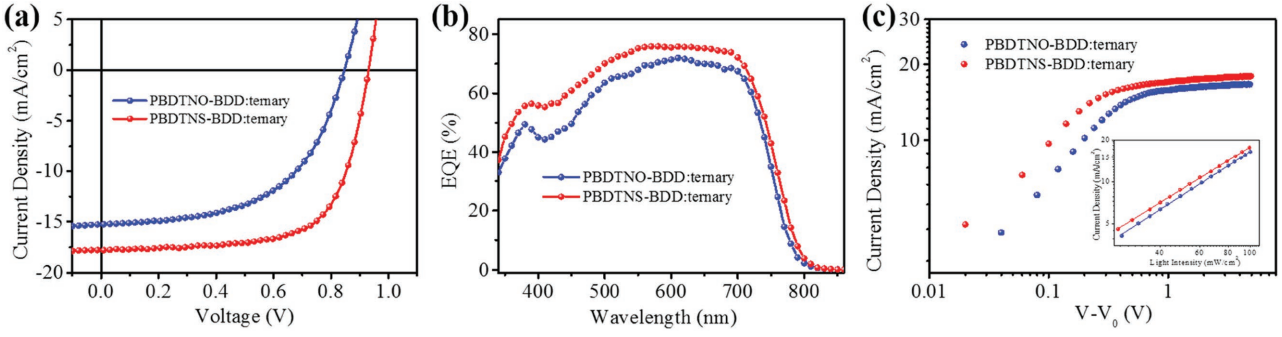

Figure 4. a) *J–V* curves of the optimal ternary devices. b) EQE spectra of the corresponding ternary devices. c) Photocurrent density (J_{ph}) versus effective voltage (V_{eff}) characteristics of the ternary devices (Inset: current density versus incident light intensity curves).

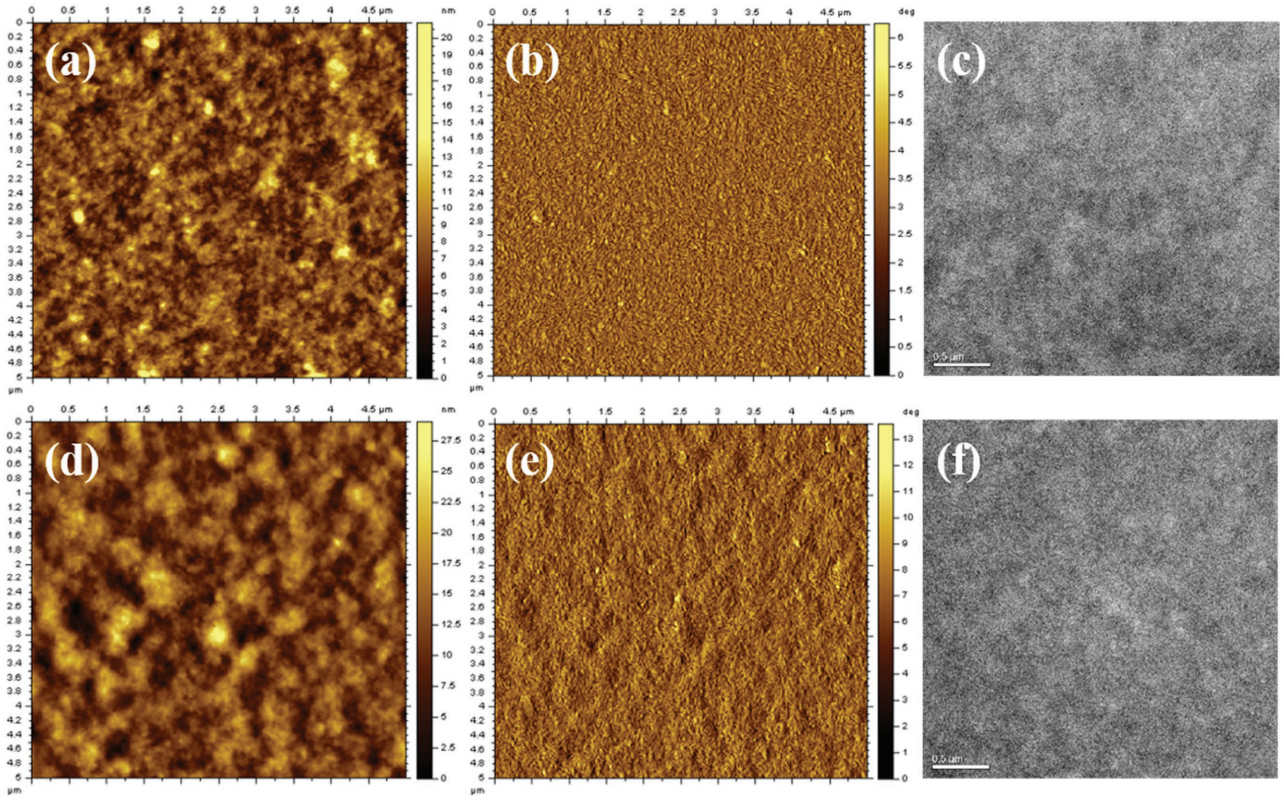

Figure 5. a) AFM height image, b) AFM phase image, and c) TEM image of PBDTNS-BDD ternary blend films. d) AFM height image, e) AFM phase image, and f) TEM image of PBDTNO-BDD ternary blend films.

and transported, and that there was room for further improvement in the current density. Interestingly, when adding a small amount of $PC_{71}BM$ into the polymer/ITIC system, the blended films dramatically changed. The RMS dropped down to 1.8 nm and 3.7 nm for PBDTNS-BDD and PBDTNO-BDD, respectively, and the films showed fibrillar interpenetrating network structures (**Figure 5**), which can be ascribed to the improvement of the miscibility, which induced a rearrangement by adding the third component $PC_{71}BM$. This favorable morphology is more strong evidence to support the remarkably high J_{SC} for ternary devices.

In this work, a new monomer containing alkylthio naphthyl was first designed and then synthesized. The resulting polymer PBDTNS-BDD showed a lower HOMO energy level than that of its alkoxyl naphthyl counterpart, PBDTNO-BDD. Surprisingly, ternary blend devices based on PBDTNS-BDD:$PC_{71}BM$:ITIC exhibited a PCE of 11.21%, which was significantly higher than that of the alkoxyl-substituted analogue-based ternary device (7.85%). Using these results an appropriate model to investigate the devices could be used to obtain useful insights. Moreover, alkylthio naphthyl holds promise as a powerful regulating unit to design desirable and highly efficient light-harvesting polymers.

Supporting Information

Supporting Information is available from the Wiley Online Library or from the author.

Acknowledgements

This work was supported by the National Natural Science Foundation of China (51773220, 51573205, 61405209, and 51673031), the Ministry of Science and Technology of China (2014CB643501). G.H. and J.Z. contributed equally to this work.

Conflict of Interest

The authors declare no conflict of interest.

Keywords

solar cells, polymers, light harvesting

Received: September 8, 2017
Revised: October 1, 2017
Published online:

[1] Y.-J. Cheng, S.-H. Yang, C.-S. Hsu, *Chem. Rev.* **2009**, *109*, 5868.
[2] Y. Li, *Acc. Chem. Res.* **2012**, *45*, 723.
[3] L. Lu, T. Zheng, Q. Wu, A. M. Schneider, D. Zhao, L. Yu, *Chem. Rev.* **2015**, *115*, 12666.
[4] L. Dou, Y. Liu, Z. Hong, G. Li, Y. Yang, *Chem. Rev.* **2015**, *115*, 12633.
[5] F. Zhao, S. Dai, Y. Wu, Q. Zhang, J. Wang, L. Jiang, Q. Ling, Z. Wei, W. Ma, W. You, C. Wang, X. Zhan, *Adv. Mater.* **2017**, *29*, 1700144.

[6] T. Kumari, S. M. Lee, S.-H. Kang, S. Chen, C. Yang, *Energy Environ. Sci.* **2017**, *10*, 258.
[7] W. Zhao, S. Li, S. Zhang, X. Liu, J. Hou, *Adv. Mater.* **2017**, *29*, 1604059.
[8] W. Zhao, S. Li, H. Yao, S. Zhang, Y. Zhang, B. Yang, J. Hou, *J. Am. Chem. Soc.* **2017**, *139*, 7148.
[9] R. A. J. Janssen, J. Nelson, *Adv. Mater.* **2013**, *25*, 1847.
[10] K. H. Hendriks, A. S. G. Wijpkema, J. J. van Franeker, M. M. Wienk, R. A. J. Janssen, *J. Am. Chem. Soc.* **2016**, *138*, 10026.
[11] L. Lu, T. Xu, W. Chen, E. S. Landry, L. Yu, *Nat. Photon.* **2014**, *8*, 716.
[12] L. Lu, M. A. Kelly, W. You, L. Yu, *Nat. Photon.* **2015**, *9*, 491.
[13] W. Chen, Z. Du, M. Xiao, J. Zhang, C. Yang, L. Han, X. Bao, R. Yang, *ACS Appl. Mater. Interfaces* **2015**, *7*, 23190.
[14] J. Hou, M.-H. Park, S. Zhang, Y. Yao, L.-M. Chen, J.-H. Li, Y. Yang, *Macromolecules* **2008**, *41*, 6012.
[15] L. Huo, S. Zhang, X. Guo, F. Xu, Y. Li, J. Hou, *Angew. Chem.* **2011**, *123*, 9871.
[16] L. Ye, S. Zhang, W. Zhao, H. Yao, J. Hou, *Chem. Mater.* **2014**, *26*, 3603.
[17] W. Chen, M. Xiao, L. Han, J. Zhang, H. Jiang, C. Gu, W. Shen, R. Yang, *ACS Appl. Mater. Interfaces* **2016**, *8*, 19665.
[18] N. Wang, W. Chen, W. Shen, L. Duan, M. Qiu, J. Wang, C. Yang, Z. Du, R. Yang, *J. Mater. Chem. A* **2016**, *4*, 10212.
[19] D. Liu, Q. Zhu, C. Gu, J. Wang, M. Qiu, W. Chen, X. Bao, M. Sun, R. Yang, *Adv. Mater.* **2016**, *28*, 8490.
[20] Q. Tao, T. Liu, L. Duan, Y. Cai, W. Xiong, P. Wang, H. Tan, G. Lei, Y. Pei, W. Zhu, R. Yang, Y. Sun, *J. Mater. Chem. A* **2016**, *4*, 18792.
[21] T. Yu, X. Xu, Y. Li, Z. Li, Q. Peng, *ACS Appl. Mater. Interfaces* **2017**, *9*, 18142.
[22] Z. Genene, J. Wang, X. Meng, W. Ma, X. Xu, R. Yang, W. Mammo, E. Wang, *Adv. Electron. Mater.* **2016**, *2*, 1600084.
[23] L. Huo, J. Hou, *Polym. Chem.* **2011**, *2*, 2453.
[24] C. Cui, W.-Y. Wong, Y. Li, *Energy Environ. Sci.* **2014**, *7*, 2276.
[25] B. Kan, Q. Zhang, M. Li, X. Wan, W. Ni, G. Long, Y. Wang, X. Yang, H. Feng, Y. Chen, *J. Am. Chem. Soc.* **2014**, *136*, 15529.
[26] B. Kan, Q. Zhang, F. Liu, X. Wan, Y. Wang, W. Ni, X. Yang, M. Zhang, H. Zhang, T. P. Russell, Y. Chen, *Chem. Mater.* **2015**, *27*, 8414.
[27] C. Cui, Z. He, Y. Wu, X. Cheng, H. Wu, Y. Li, Y. Cao, W.-Y. Wong, *Energy Environ. Sci.* **2016**, *9*, 885.
[28] H. Kim, B. Lim, H. Heo, G. Nam, H. Lee, J. Y. Lee, J. Lee, Y. Lee, *Chem. Mater.* **2017**, *29*, 4301.
[29] X. Gong, G. Li, C. Li, J. Zhang, Z. Bo, *J. Mater. Chem. A* **2015**, *3*, 20195.
[30] J.-H. Kim, C. E. Song, B. Kim, I.-N. Kang, W. S. Shin, D.-H. Hwang, *Chem. Mater.* **2014**, *26*, 1234.
[31] J. Wang, M. Xiao, W. Chen, M. Qiu, Z. Du, W. Zhu, S. Wen, N. Wang, R. Yang, *Macromolecules* **2014**, *47*, 7823.
[32] M. Zhang, X. Guo, W. Ma, S. Zhang, L. Huo, H. Ade, J. Hou, *Adv. Mater.* **2014**, *26*, 2089.
[33] H. Yao, H. Zhang, L. Ye, W. Zhao, S. Zhang, J. Hou, *Macromolecules* **2015**, *48*, 3493.
[34] D. Ding, J. Wang, Z. Du, F. Li, W. Chen, F. Liu, H. Li, M. Sun, R. Yang, *J. Mater. Chem. A* **2017**, *5*, 10430.
[35] T. Liu, L. Huo, X. Sun, B. Fan, Y. Cai, T. Kim, J. Y. Kim, H. Choi, Y. Sun, *Adv. Energy Mater.* **2016**, *6*, 1502109.
[36] D. Baran, R. S. Ashraf, D. A. Hanifi, M. Abdelsamie, N. Gasparini, J. A. Rohr, S. Holliday, A. Wadsworth, S. Lockett, M. Neophytou, C. J. Emmott, J. Nelson, C. J. Brabec, A. Amassian, A. Salleo, T. Kirchartz, J. R. Durrant, I. McCulloch, *Nat. Mater.* **2017**, *16*, 363.
[37] G. Zhang, K. Zhang, Q. Yin, X. F. Jiang, Z. Wang, J. Xin, W. Ma, H. Yan, F. Huang, Y. Cao, *J. Am. Chem. Soc.* **2017**, *139*, 2387.
[38] F. Zhao, Y. Li, Z. Wang, Y. Yang, Z. Wang, G. He, J. Zhang, L. Jiang, T. Wang, Z. Wei, W. Ma, B. Li, A. Xia, Y. Li, C. Wang, *Adv. Energy Mater.* **2017**, *7*, 1602552.
[39] J. Zhang, Y. Zhang, J. Fang, K. Lu, Z. Wang, W. Ma, Z. Wei, *J. Am. Chem. Soc.* **2015**, *137*, 8176.
[40] H. Lu, J. Zhang, J. Chen, Q. Liu, X. Gong, S. Feng, X. Xu, W. Ma, Z. Bo, *Adv. Mater.* **2016**, *28*, 9559.
[41] C. Wang, X. Xu, W. Zhang, S. B. Dkhil, X. Meng, X. Liu, O. Margeat, A. Yartsev, W. Ma, J. Ackermann, E. Wang, M. Fahlman, *Nano Energy* **2017**, *37*, 24.
[42] G. Li, V. Shrotriya, J. Huang, Y. Yao, T. Moriarty, K. Emery, Y. Yang, *Nat. Mater.* **2005**, *4*, 864.
[43] J.-L. Wu, F.-C. Chen, Y.-S. Hsiao, F.-C. Chien, P. Chen, C.-H. Kuo, M. H. Huang, C.-S. Hsu, *ACS Nano* **2011**, *5*, 959.

